Available online at www.sciencedirect.com
ScienceDirect
Trans. Nonferrous Met. Soc. China 20(2010) s540−s544
Transactions of Nonferrous Metals Society of China
www.tnmsc.cn

High temperature tensile behaviors of extruded and rolled AZ31 Mg alloy

QIAO Jun(乔 军), WANG Yu(王 瑜), SHI Guo-dong(史国栋)

College of Materials Science and Engineering, University of Science and Technology Liaoning, Anshan 114051, China

Received 23 September 2009; accepted 30 January 2010

Abstract: High temperature tensile ductilities and deformation mechanisms of an extruded and rolled AZ31 Mg alloy were investigated. Elongation-to-failure tests were conducted under constant T-head velocity and constant temperatures ranging from 300 ˚C to 450 ˚C. Strain-rate-change tests were conducted under varying strain rate from 5×10^{-5} s^{-1} to 2×10^{-2} s^{-1} and constant temperature from 300 ˚C to 450 ˚C. Experimental results show that the maximum elongation of the AZ31 alloy with an average grain size of about 19 μm is 117% at strain rate of 10^{-3} s^{-1} and temperature of 450 ˚C. Stress exponent and activation energy were characterized to clarify the deformation mechanisms. The enhanced ductility is dominated by solute drag dislocation creep, and the major failure mechanism is cavity growth and interlinkage.

Key words: AZ31 Mg alloy; solute-drag creep; tensile ductility; superplasticity; stress exponent

1 Introduction

In recent years, magnesium alloys are widely applied because of their advantages of low density, high specific strength and strong corrosion resistance, etc. Compared with casting Mg alloys, deformed Mg alloys offer higher strength and ductility, and better comprehensive mechanical properties which allow their extensive application in aerospace, transportation and electrocommunication etc[1].

Hot or warm deformation is a significant technique for further processing of Mg alloy sheets. High temperature deformation is generally viewed as following a power-law relationship between the creep rate $\dot{\varepsilon}$ and flow stress σ, as given in the phenomenological equation for creep[2]:

$$\dot{\varepsilon} = A\left(\frac{\sigma}{E}\right)^n \exp\left(-\frac{Q}{RT}\right) \quad (1)$$

where A is material constant related to stacking fault energy; E is dynamic elastic modulus; n is stress exponent, commonly taking values from 2 to 8; Q is activation energy for creep; R is gas constant; and T is absolute temperature.

High-temperature formability of Mg alloys can be enhanced through following mechanisms: 1) activated new slip system on prism plane[3]; 2) grain refinement by dynamic recrystallization[4−5]; 3) fine-grained superplasticity (n=2)[6−7]; and 4) dislocation creep (n=3−8)[8−11]. SOMEKAWA et al[9] show that tensile deformation from 200 ˚C to 350 ˚C was dominated by dislocation-climb creep accompanied by either lattice diffusion at high temperatures where n=5 or pipe diffusion at low temperatures where n=7. While WATANABE et al[10] studied AZ 31 alloy at the similar stress level and temperature from 325 ˚C to 400 ˚C and concluded that creep deformation with n=3.3 was dominated by solute-drag creep, and ZHANG et al[11] showed that when temperature was higher than 420 ˚C, low-stress creep behavior of an AZ31 alloy with n=2.7 was dominated by either dislocation-climb creep or solute-drag creep. However, the deformation conditions for solute-drag creep and dislocation-climb creep, the transition between them, and the function of dynamic recrystallization during dislocation creep are not clarified.

In the present study, tensile behaviors of an extruded and rolled AZ31 Mg alloy were investigated under different temperatures and strain rates. The deformation mechanism, microstructure and failure mechanism were analyzed and discussed.

Foundation item: Project(50801034) supported by the National Natural Science Foundation of China; Project(20060425) supported by the Scientific and Technological Research Key Lab Foundation of Liaoning Education Department, China

Corresponding author: QIAO Jun; Tel: +86-412-5929532; E-mail: qiaoj@ustl.edu.cn

2 Experimental

An AZ31 casting bar of d=165 mm was extruded to a plate with thickness of 12 mm, and then the thickness was reduced to 5.5 mm through three-pass hot rolling. The chemical compositions of the AZ31 alloy are given in Table 1.

Table 1 Chemical compositions of AZ31 alloy (mass fraction, %)

Al	Mn	Zn	Be	Cu	Fe	Si	Mg
3.19	0.334	0.81	0.01	0.005	0.005	0.02	Bal.

High-temperature mechanical tests of elongation-to-failure (EF) test and strain-rate-change (SRC) test were conducted on a MTS810 machine facilitated with a split resistance furnace controlled within ±3 ˚C. A thermal couple was attached to the specimen located in the middle of the soaking zone of the furnace. Each specimen was preheated for 15 min in the furnace before the mechanical tests to stabilize the temperature and the testing system.

As the specimen geometry shown in Fig.1, the thickness and tensile axis of each specimen correspond to the plate thickness and the rolling direction, respectively. Before the mechanical tests, some specimens wrapped with aluminium foil were annealed at 400 ˚C for 2 h in a resistance furnace, followed by air cooling. EF tests for both of the original specimens and the annealed specimens were conducted at constant temperature ranging from 300 ˚C to 450 ˚C and constant crosshead velocity of 2.54×10^{-5} and 2.54×10^{-4} m/s until the specimen failed. SRC testes were conducted at constant temperature ranging from 300 ˚C to 450 ˚C, at which a prestrain of about 15% at a low rate was applied to stabilize the testing system, followed by nine continuous stages with the increase of strain rate from 5×10^{-5} s^{-1} to 2×10^{-2} s^{-1}. Flow stress and true strain rate at each stage were calculated based on SRC data, and stress exponent at each temperature was regressed according to Eq.(1).

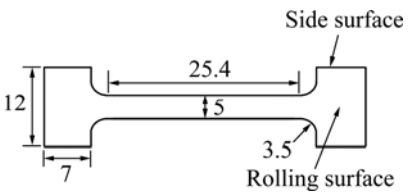

Fig.1 Specimen geometry for high-temperature mechanical test (Unit: mm)

Metallographic pieces taken from the as-received plate and the specimens after elongation-to-failure (EF) tests were prepared, ground, and etched in a solution of 4.2 g trinitrophenol, 10 mL acetic acid, 70 mL alcohol, and 10 mL water for about 8 s. Grain boundaries and failure features were observed under an optical microscope of JVC TK-350EG, and linear intercept method was applied to measure grain size.

3 Results

Two metallographs for the rolling plane and the side plane of the as-received alloy are shown in Fig.2 (vertically in rolling direction). Compared with the typical extruded pattern shown in Fig.2(b), texture near rolling surface with an average grain size of d=19 μm presents more equiaxed grain distribution, as shown in Fig.2(a).

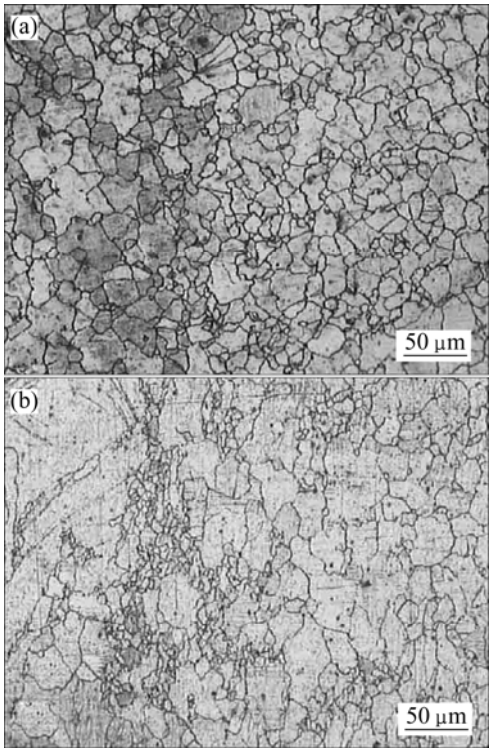

Fig.2 Optical micrographs of as-received AZ31 alloy: (a) Rolling plane; (b) Side plane

Data of EF tests for both the original and the annealed specimens are shown in Fig.3(a). As predicted, tensile strength increases with the increase of strain rate. The two original specimens show an obvious strain-softening behavior while the annealed specimen exhibits a much longer steady-state deformation. Fig.3(b) shows the measured elongations at strain rate of 10^{-3} s^{-1} and temperature from 300 ˚C to 450 ˚C. Although EF percentage at 300 ˚C and 350 ˚C is 52.04% and

84.64%, respectively, the material exhibits excellent tensile ductilities of over 100% at 400 ˚C and 450 ˚C.

Elongations under constant strain rate of 10^{-3} s^{-1} is shown in Fig.4, in which D_0=5×10^{-5} m^{-2}/s[12], and Q=136 kJ/mol[13]. The compensation of strain rate, $\dot{\varepsilon}/D$, is similar to the Zener-Hollomon parameter, which accounts for the temperature dependence of diffusivity. The maximum elongation of 117% is achieved at 450 ˚C and diffusivity-compensated strain rate of 4.5×10^8 m^{-2}.

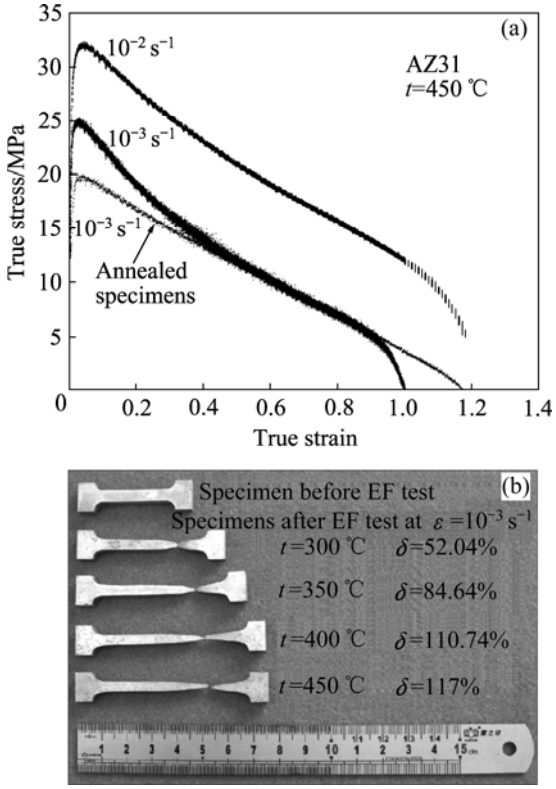

Fig.3 EF test data: (a) Stress—strain curves at t=450 ˚C; (b) Elongations at stain rate of 10^{-3} s^{-1} and different temperatures

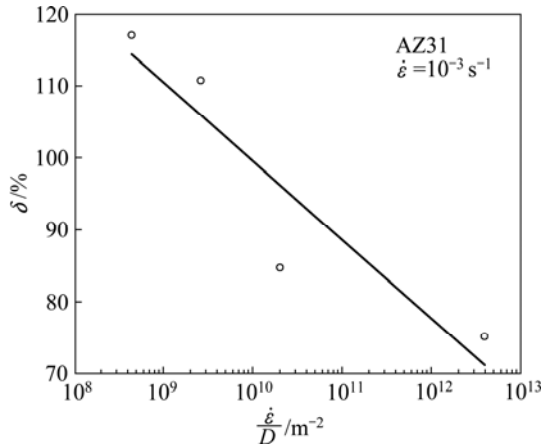

Fig.4 Elongations under constant strain rate of 10^{-3} s^{-1}

Most of the EF specimens exhibit necking before failure. Optical micrographs of a failed specimen after EF test at 450 ˚C and 10^{-3} s^{-1} are shown in Fig.5. It is shown in Figs.5(a) and (b) that the grains in the gage region are elongated along the tensile direction and fine grains develop around grain boundaries. Figs.5(c) and

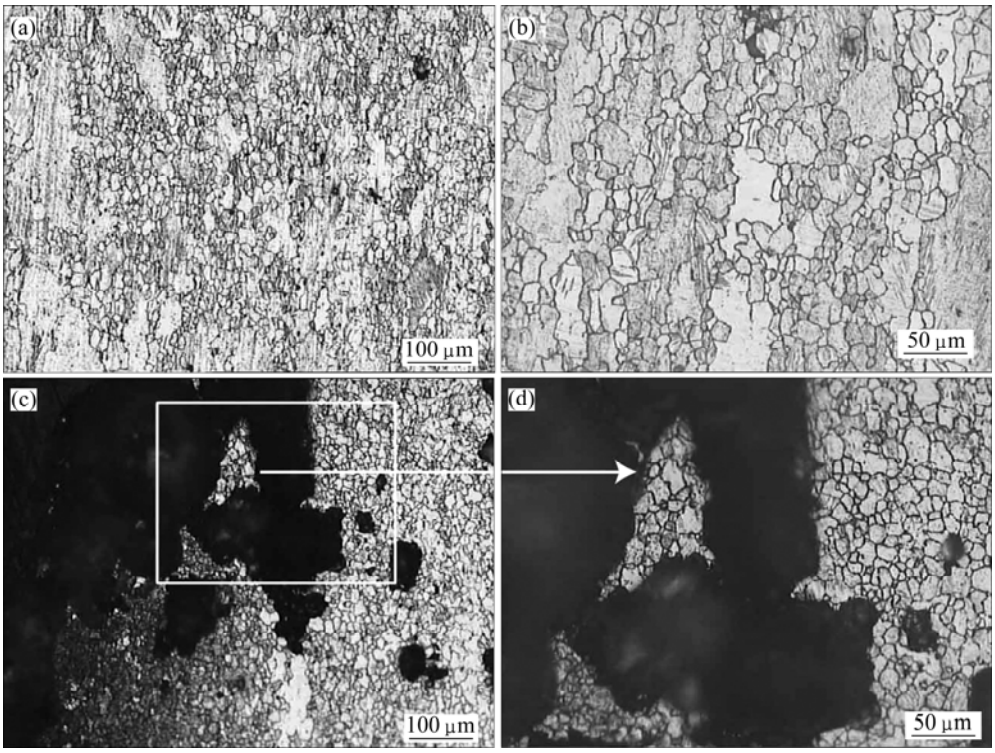

Fig.5 Optical micrographs of specimen after EF test at 450 ˚C and 10^{-3} s^{-1} (in vertical tensile direction): (a), (b) Gage point far from failure end; (c), (d) Failure end

(d) show the micrographs of the failure end where cavities with a size of about 50 μm are apparent. The shape of the failure end is consistent with the jagged failure surface, which indicates that cavity growth and interlinkage cause the sample failure. The cavities are typically nucleated at particles or grain boundaries. The measured average grain size is d = 11.00 μm for the gage point, and d=10.67 μm for the failure end (d=1.74 L, L is the linear intercept size). The newly developed fine grains are resulted from dynamic recrystallization during high-temperature deformation.

SRC data of the AZ31 material are shown in Fig.6 as strain rate against modulus-compensated flow stress in dual-logarithmic scale. The dynamic, unrelaxed modulus is taken equal to the data in Ref.[9]. The linear trend at each temperature in Fig.6 indicates the relationship between strain rate and flow stress, and the slope at each temperature is equal to the stress exponent. It is obvious that the alloy presents the highest strength and stress exponent at 300 ˚C.

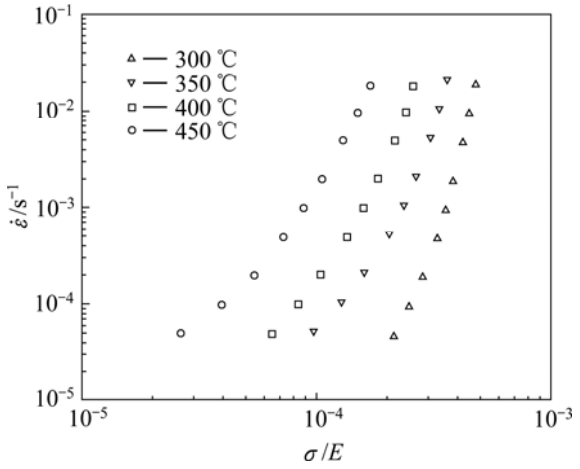

Fig.6 SRC test data plotted as true strain rate versus modulus-compensated flow stress

4 Discussion

Based on the phenomenological equation for creep, strain rates in Fig.6 are compensated by diffusivity of Al in Mg, as shown in Fig.7. A master curve reflecting both strain rate and temperature is generated and used to analyze deformation mechanism.

In the region of high temperature and low strain rate, low $\dot{\varepsilon}/D$ range from 3×10^{9} m^{-2} to 5×10^{10} m^{-2}, the stress exponent is close to 3. With the increase of strain rate and decrease of temperature, stress exponent increases to about 5 during $\dot{\varepsilon}/D$ range from 7×10^{10} m^{-2} to 2×10^{12} m^{-2}. While in the range of low temperature and high strain rate, $4\times10^{12}\leq\dot{\varepsilon}/D\leq2\times10^{14}$ m^{-2}, stress exponent n is about 7. Calculated stress exponents at each temperature are shown in Table 2. The increasing

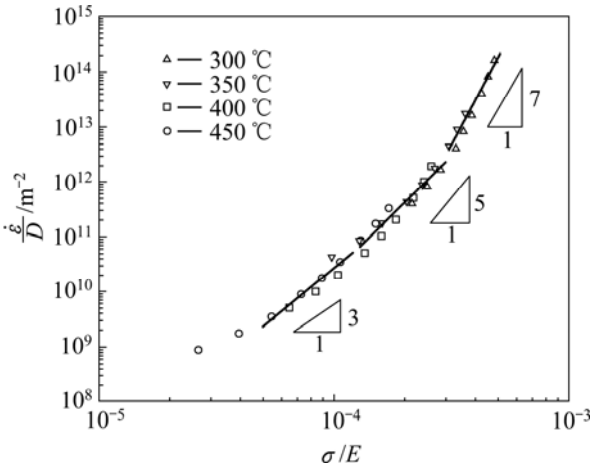

Fig.7 SRC test data plotted as diffusivity-compensated strain rate versus modulus-compensated flow stress

Table 2 Calculated stress exponents

Temperature/°C	300	350	400	450
n	7.51	4.53	4.20	3.23

stress exponent with increasing $\dot{\varepsilon}/D$ may reflect the changing deformation mechanism from solute-drag creep (n is about 3) to dislocation-climb creep (n is about 5 or 7)[9].

At low strain rate and high temperature, solute atoms are able to diffuse and interact with the stress field of edge dislocations. This interaction keeps exerting a dragging force on gliding dislocation and causes the gliding to be the dominate one in the sequential process of gliding and climbing. The activation energy was calculated according to the following equation:

$$Q=\left[\frac{nR\partial\ln\sigma}{\partial(1/T)}\right]_{\dot{\varepsilon}} \tag{2}$$

where $\dot{\varepsilon}$ is creep rate[14]. As shown in Fig.8, the calculated activation energy at 450 ˚C and 10^{-3} s^{-1} is Q=141.12 kJ/mol, which is similar to the diffusional activation energy of Al in Mg, Q=(143±10) kJ/mol[14−15]. Based on the calculated activation energy and stress exponent, the tensile deformation at 450 ˚C is rate controlled by solute-drag creep.

The increase of stress exponent shown in Fig.7 reflects a decrease of creep activation energy. When n is about 5 or 7, with the increase of strain rate and decrease of temperature, the interaction between solute atmosphere and dislocation is weaken, and dislocation climbing becomes the slower and creep-rate dominated one between the sequential gliding and climbing process. The activation energy for climb-controlled creep is close to that for lattice diffusion[9].

The finer grains after EF test shown in Fig.5 results from dynamic recrystallization during high temperature deformation. This fine structure can contribute to tensile ductility by grain-boundary-sliding (GBS) mechanism. KOTTADA et al[16] calculated the contribution of GBS to strain for a Mg-0.7%Al alloy and concluded that new slip system activated by increasing stress caused a transfer from diffusional creep to dislocation creep, and the contribution of GBS to total strain correspondingly decreased. Considering the deformation conditions in this study, the fact that the cavity development during EF tests and the calculated stress exponent, the dominate creep mechanism in this study is dislocation creep other than diffusional creep. From the dislocation creep, particularly solute-drag creep, enhanced tensile ductility of over 100% are consistently achieved for the AZ31 alloy at 400 ˚C and 450 ˚C.

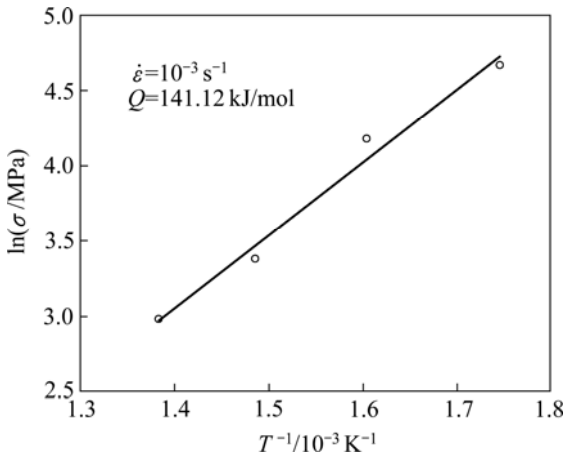

Fig.8 Calculation of creep activation energy

5 Conclusions

1) Tensile ductilities of over 100% are achieved at temperature of 450 ˚C and strain rate of 10^{-3} s^{-1} for the extruded and rolled AZ31 alloy. The dominate deformation mechanism for this enhanced tensile ductilities is solute-drag creep with a stress exponent of 3.23 and activation energy of 141.21 kJ/mol.

2) The failure mechanism of the EF specimens is cavity growth and interlinkage. Fine grains are developed from dynamic recrystallization during EF tests, but the contribution of GBS to the final strain is limited by the applied test conditions and the corresponding cavity growth.

3) For the extruded and rolled AZ31 alloy, initial annealing is preferred to avoid strain softening during tensile test. Annealed specimens exhibit longer steady-state tensile process which is preferred for high-temperature mechanical tests.

References

[1] YU K, RUI S T, SONG J M, LI W X, GUO L. Effects of grain refinement on mechanical properties and microstructures of AZ31 alloy [J]. Transaction of Nonferrous Metals Society China, 2008, 18(z1): 39−43.

[2] MUKHERJEE A K. An examination of the constitutive equation for elevated temperature plasticity [J]. Materials Science and Engineering A, 2002, 322(1/2): 1−22.

[3] ITO T, SAEKI J, OTSUKA M. Superplastic-like behavior in coarse grained Mg-Al solid solutions [J]. J Japan Inst Metals, 2003, 67(2): 85−92.

[4] ZHANG Yan-shu, ZENG Zhi-peng, JIN Quan-lin. Hot forming behavior and microstructure evolution of magnesium alloy AZ31D [J]. Metal Heat Proceessing, 2007, 32(7): 22−26. (in Chinese)

[5] VALLE J A D, RUANO O A. Separate contributions of texture and grain size on the creep mechanisms in a fine-grained magnesium alloy [J]. Acta Materialia, 2007, 55(2): 455−466.

[6] CAO Jian, ZHANG Fu-quan, XIA Wei-jun, FU Ding-fa, CHEN Zhen-hua, WU You-wu. Superplasticity in a rolled AZ31 magnesium alloy by multi-stage deformation [J]. Light Metal, 2005, 2: 58−61. (in Chinese)

[7] DEL VALLE J A, PEREZ-PRADO M T, RUANO O A. Deformation mechanisms responsible for the high ductility in a Mg AZ31 alloy analyzed by electron backscattered diffraction [J]. Metallurgical and Materials Transactions A, 2005, 36(6): 1427−1438.

[8] ZHANG Shi-chang, ZHU Ming, ZHAO Gang, CHEN Chang-jun. Effect of zinc content on high temperature creep property of AZ31 magnesium alloy [J]. The Chinese Journal of Nonferrous Metals, 2008, 18(7): 1205−1210. (in Chinese)

[9] SOMEKAWA H, HIRAI K, WATANABE H, TAKIGAWA Y, HIGASHI K. Dislocation creep behavior in Mg-Al-Zn alloys [J]. Materials Science and Engineering A, 2005, 407(1/2): 53−61.

[10] WATANABE H, TSUTSUI H, MUKAI T, KOHZU M, TANABE S, HIGASHI K. Deformation mechanism in a coarse-grained Mg-Al-Zn alloy at elevated temperatures [J]. International Journal of Plasticity, 2001, 17(3): 387−397.

[11] ZHANG Shi-chang, ZONG Qin, HU Yan-sheng, CHENG Xiao-ru. Creep property and mechanism of AZ31 magnesium alloy under high temperature and low stress [J]. Mechanical Engineering, 2009, 45(3): 291−295. (in Chinese)

[12] FUNAMIZU Y, WATANABE K. Interdiffusion in the Al-Mg system [J]. Trans JIM, 1972, 13(4): 278−283.

[13] MCNELLEY T R, MICHEL D J, SALAMA A. The Mg-concentration dependence of the strength of Al-Mg alloys during glide-controlled deformation [J]. Scripta Metall, 1989, 23(10): 1657−1662.

[14] CHEN Hui-qin, CAO Chun-xiao, GUO Ling, LIN Hai. Hot deformation mechanism and microstructure evolution of TC11 titanium alloy in β field [J]. Transactions of Nonferrous Metals Society of China, 2008, 18(5): 1021−1027.

[15] VAGARALI S S, LANGDON T G. Deformation mechanisms in h.c.p. metals at elevated temperatures-II. Creep behavior of a Mg-0.8%Al solid solution alloy [J]. Acta Metallurgica, 1982, 30(6): 1157−1170.

[16] KOTTADA R S, CHOKSHI A H. Grain boundary sliding during diffusion and dislocation creep in a Mg-0.7 Pct Al alloy [J]. Metallurgical and Materials Transactions A, 2007, 38(8): 1743−1749.

(Edited by CHEN Can-hua)